Available online at www.sciencedirect.com
SCIENCE DIRECT
International Journal of Coal Geology 67 (2006) 191–201
International Journal of COAL GEOLOGY
www.elsevier.com/locate/ijcoalgeo

Combustion studies in a fluidised bed—The link between temperature, NO_x and N_2O formation, char morphology and coal type

B. Valentim [a,*], M.J. Lemos de Sousa [a], P. Abelha [b], D. Boavida [b], I. Gulyurtlu [b]

[a] *Centro de Geologia da Universidade do Porto, Faculdade de Ciências, Praça de Gomes Teixeira, 4099-002, Porto, Portugal*
[b] *Departamento de Engenharia Energética e Controlo Ambiental (DEECA), Instituto Nacional de Engenharia, Tecnologia e Inovação (INETI), Estrada do Paço do Lumiar, 22, Edif. J, 1649-038, Lisboa, Portugal*

Received 29 January 2004; accepted 4 November 2005
Available online 3 March 2006

Abstract

Five commercially available high volatile bituminous coals from different origins were studied with the objective of characterizing their petrographic nature with respect to emissions of NO_x and N_2O. The chars produced [at temperatures ranging from 700 to 1000 °C] from these coals were also petrographically analyzed to assess the contribution of char to NO_x and N_2O formation during combustion.

Vitrinite-rich coals produced higher porous chars (cenospheres and tenuinetworks) than those that are rich in inertinite. The former coals were, however, found to release lower concentrations of NO.

Consistent with previous works, N_2O emissions were observed to decrease significantly with temperature, however, on the whole, the N_2O emissions from vitrinite-rich high volatile coals were less than those from inertinite-rich coals. Additionally, high porous chars were found to give rise to lower emissions of NO and N_2O.

Keywords: Coal; Petrography; Microlithotype; Char morphotype; NO_x; N_2O; Fluidised bed combustion (FBC)

1. Introduction

Fluidised bed combustion (FBC) is a technique that allows the combustion of coal with the production of low NO_x and SO_x emissions. However, because standard operating conditions favor lower SO_2 formation, substantial N_2O can be produced during fluidised bed combustion and N_2O significantly contributes to the greenhouse effect and also to the depletion of the ozone layer (IEA/OECD, 1999; Jacobson, 2002).

In FBC, coal devolatilization occurs in less than 1 s, while the oxidation of the char may last for several minutes. During coal combustion, the fuel-N is divided between the volatiles, the tar, and the char, and the availability of oxygen is mainly responsible for the reduced release of nitrogen oxides. For this reason, and due to the low operation temperatures used in FBC, almost all oxides of nitrogen are formed from the reaction of coal–nitrogen with oxygen, leading to the formation of NO_x and N_2O, with the latter decreasing as

* Corresponding author. Tel.: +351 220114524.
E-mail address: bvvalent@fc.up.pt (B. Valentim).

0166-5162/$ - see front matter © 2006 Elsevier B.V. All rights reserved.
doi:10.1016/j.coal.2005.11.010

combustion temperature increases, whereas NO_x exhibits the opposite trend (Molina et al., 2000). However, there are also variations in nitrogen oxide release originating from coal properties, such as rank, maceral composition, and mineral matter (Shimizu et al., 1992; Gavin and Dorrington, 1993; Pels et al., 1993; Wang et al., 1994).

The nitrogen present in coal is almost exclusively associated with the organic matter, usually in the range 0.7–2.1 wt.% (dmmf), with an average amount of ≈1.5 wt.% (dmmf) in bituminous coals (Burchill and Welch, 1989). It is stated that the nitrogen presence decreases with petrographic nature in the order: vitrinite > semifusinite > inertinite (Hindmarsh et al., 1994). XPS analysis of parent coals and chars identified that nitrogen functionalities in coal are basically pyrrolic (50–80%), pyridinic (20–40%) and quaternary nitrogen (0–20%). Small amounts (10%) of amino groups may be present in low rank coals. (Molina et al., 2000).

The relation between coal macerals and NO_x formation was studied by several authors (Brown and Thomas, 1993; Crelling et al. 1993; Gonzáles de Andrés and Thomas, 1994; Wang et al., 1994; Harding et al. 1996). The latter studies mainly involved controlled-temperature thermogravimetric technique, using a wide range of coals and chars prepared from them in an entrained-flow reactor. It has been found that the maceral and microlithotype composition determines the char morphology, the NO emissions, char reactivity, and surface area, which also have a direct influence on NO emissions (Brown and Thomas, 1993; Crelling et al., 1993; Wang et al., 1994; Varey et al., 1996). Previous studies in fluidised beds (Shimizu et al., 1992; Gavin and Dorrington, 1993; Pels et al., 1993; Xie et al., 2001) have also demonstrated the importance of coal properties in the oxidation and reduction of coal-N and char-N.

This paper reports the results of a research work on the release of nitrogen oxides from a set of five iso-rank coals, differing in their origin and maceral composition. The studies were carried out in a fluidised bed combustor.

2. Methods and material studied

2.1. Coal samples

Five commercially available high-volatile bituminous coals with different maceral composition were used in this study to produce chars and for combustion trials. They included a vitrinite-rich Colombian coal, a vitrinite-rich U.S. coal, and three inertinite-rich South African coals. The codes for the coals used in this study are given in Table 1.

2.1.1. Coal analytical characterization data

Proximate analysis of the coals was determined by ASTM D3173-73 (1984, moisture), ASTM D3175-89 (volatile matter), ASTM D3174-89 (ash) and ASTM D3172 (fixed carbon). The ultimate analysis of the coals was carried out on an Elemental Analyzer Perkin Elmer.

After the preparation of a classical coal particulate block (ISO Standard 7404-2), coal petrographic analyses (Vitrinite reflectance, Maceral group and Microlithotype composition, in accordance with ISO 7404-5, 7404-3, 7404-4, respectively) were performed on a MPV-C Leitz microscope with magnifications up to ×500 using the Leitz MPVGEOR computer program.

The microlithotype composition analysis was also undertaken, according to microlithotype classifications that were previously proposed for pulverized fuel (p.f.)

Table 1
Coal proximate and ultimate analysis

Sample origin	SA1 South Africa	Col Colombia	SA2 South Africa	SA3 South Africa	EUA U.S.
Proximate analysis (wt.%)					
Ash (dry)	10.2	8.9	14.1	16.5	14.0
Volatile matter (daf)	35.9	42.4	34.7	27.8	39.3
Fixed carbon (daf)	64.1	57.7	64.9	72.2	60.7
Ultimate analysis (wt.%)					
C (daf)	80.5	82.0	77.0	79.0	84.9
H (daf)	5.0	5.8	5.0	4.4	5.1
N (daf)	2.1	1.6	1.7	1.7	1.5
S (daf)	0.8	0.9	0.8	0.6	1.1
O[a]	11.7	9.7	15.4	14.2	7.4

[a] By difference.

conditions by Rosenberg et al. (1996) and Diessel (1998), relating microlithotypes to specific char morphotypes:

- Microlithotypes precursors of Group 1 chars, i.e., high porous chars (MPG1): Vitrite + Liptite + Clarite-V + Clarite-E + Vitrinertite-V + Trimacerite-V + Trimacerite-E;
- Microlithtypes precursors of Group 2–3 chars, i.e., mean and low porous chars (MPG2-3): Inertite + Vitrinertite-I + Durite-I + Durite-E + Trimacerite-I.

2.1.2. Char sample preparation in a fluidised bed reactor

Chars were obtained through the devolatilization of coals used in a fluidised bed reactor with 80 mm internal diameter and 500 mm of height. The inert carrier gas used in all tests was N_2. During the volatile release, CO and CO_2 amounts were monitored with non-dispersive infra-red analyzers and, when the analyzers could no longer detect these gases, the heating was switched off while maintaining the N_2 flow. Chars were produced at four different temperatures (700, 800, 900, and 1000 °C), with a heating rate of ca. 10^4 K/s, and coal particle sizes of 500–1000 μm.

2.1.3. Char analytical characterization data

Ultimate analyses of the chars produced were carried out using a LECO CNHS-932 and LECO CNH-2000 analyzers.

Char samples for petrographic analysis were prepared according to the technique presented by Álvarez (1996). Char petrographic analyses were performed with a light reflection Nikon microscope, with ×80 total magnification, and coupled with a Swift F 415C semi-automatic point-counter. Char particles were classified and counted, as described in Table 2, based on the classification developed by Bailey et al. (1990), Bailey (1994), Álvarez et al. (1997) and Sorensen et al. (2000).

2.1.4. Fluidised bed combustion measurements

Combustion tests of coals were carried out in an electrically heated fluidised bed with 80 mm internal diameter and 500 mm height. The inert bed material was constituted by silica sand with an average particle size of 370 μm.

The combustion temperature was varied in the range of 700–1000 °C, and was controlled automatically by a Eurotherm controller. The bed temperature was continuously monitored with a type-K thermocouple.

The combustion gases, after being filtered and dried, were continuously analyzed at the exit of the combustor, with specific on-line analyzers, which were previously calibrated. A paramagnetic method was employed for O_2 measurements and a non-dispersive infrared technique was used to determine the amounts of CO, CO_2, and N_2O. The NO_x and SO_2 measurements were carried out with chemiluminescence and pulsed-fluorescence analyzers, respectively.

Table 2
Simplified char classification system for FBC

Char morphotype	Description
Tenuisphere	Spheric to angular shape, porosity >80% and 75% of the wall <30 μm.
Crassisphere	Spheric to angular shape, porosity >60% and 75% of the wall >30 μm.
Tenuinetwork	Internal network structure, porosity >70% and 75% of the wall <30 μm.
Crassinetwork	Internal network structure, porosity 40–70% and 75% of the wall >30 μm.
Mixed	Char with fused and unfused regions, porosity 40–70%. Fused or unfused regions never less than 25%.
Solid	Dense, porosity 5–40%, 75% of the wall >50 μm; inertoids, fusinoids or solids <5% porosity.
Fragment	Other morphotype fragments <1000 μm^2
Classification in groups (Bailey et al., 1990; Diessel, 1998)	
Group 1	Tenuispheres + Crassispheres + Tenuinetworks + Fused fragments
Group 2–3	Crassinetworks + Mixed + Solid + Unfused fragments

3. Results and analyses

3.1. Coal characterization studies

Table 1 shows the results of the proximate and ultimate analyses of the coals and the results of coal petrography are presented in Table 3.

In accordance with ASTM D 388 and Damberger et al. (1984) all coals are reasonably similar in rank, having vitrinite reflectance in the range 0.63–0.82Rr% and volatile matter of 27.8–42.4 wt.% (daf). The lowest nitrogen value determined was 1.5 wt.% (daf) for EUA coal and the highest was 2.1 wt.% (daf) for SA1 coal (Table 1).

It is worth to mention that the large volatile matter range is essentially due to fact that the South African coals are inertinite-rich while the Colombian and the USA coals are vitrinite-rich coals. Additionally, the discrepancy between the reflectance value (0.63%Rr) and the volatile matter value (27.8 wt.%, daf) found for SA3 coal is also due to the high amount of inertinite.

The petrographic analysis revealed that EUA and Col coals are vitrinite-rich and SA1, SA2 and SA3 are inertinite-rich.

Table 3
Results of vitrinite mean random reflectance (Rr%), maceral and microlithotype analysis (vol.%)

Sample:	SA1	Col	SA2	SA3	EUA
Rr	0.63	0.64	0.64	0.65	0.82
Vitrinite	40	83	39	13	65
Liptinite	5	3	4	5	10
Inertinite	51	13	53	76	21
Minerals	4	1	4	6	4
V+L[a]	45	86	43	18	75
Reactive[b]	50	88	48	25	76
Non-reactive	46	11	48	69	20
Vitrite	23	53	19	5	31
Liptite	0	0	0	0	1
Inertite	30	3	33	60	4
Clarite V	3	9	5	1	16
Clarite E	0	0	0	0	2
Vitrinertite V	8	24	6	4	8
Vitrinertite I	8	3	6	6	1
Dutrite I	7	0	10	12	5
Dutrite E	0	0	1	0	3
Trimacerite V	7	6	8	1	13
Trimacerite I	6	0	4	3	6
Trimacerite E	0	0	0	0	2
Carbominerite	6	1	6	6	7
Minerite	2	0	1	1	2
MPG1—microlithotypes precursors of Group 1 chars[c]	42	92	38	12	72
MPG2–3 microlithotypes precursors of Group 2 and 3 chars[d]	51	7	54	81	19

[a] Vitrinite + Liptinite.
[b] Vitrinite + Liptinite + 30% of the semifusinite.
[c] (Vitrite + Liptite + Clarite-V + Clarite-E + Vitrinertite-V + Trimacerite-V + Trimacerite-E).
[d] (Inertite + Vitrinertite-I + Durite-I + Durite-E + Trimacerite-I).

The EUA coal presents high amounts of collotelinite associated with sporinite and cutinite. For this reason, the microlithotype composition of this coal is dominated by vitrite, clarite, and vitrinertite-V (Table 3).

The Col coal has an abundance of desmocollinite and a microlithotype composition almost all composed of vitrite and vitrinertite-V (Table 3). The petrographic analysis has also shown the presence of a large amount of bind fine coal (Valentim et al., 2006-this volume).

SA1 and SA2 coals are inertinite-rich coals, with vitrinite amounts of ca. 40% and abundant semifusinite. The microlithotype composition of these coals is dominated by inertite, and vitrite, with lesser amounts of vitrinertite-V-I and durite-I (Table 3).

SA3 has high amounts of inertinite, with 60% inertite and 12% durite-I (Table 3).

From the results presented in Table 3 it can be seen that Col and EUA coals are MPG1-rich and SA1, SA2 and SA3 coals are MPG2-3-rich.

3.2. Char characterization studies

The characterization data for chars produced during devolatilization in the fluidised bed are given in Tables 4–6.

The nitrogen content of the char was found to be comparable to that of the parent coal as shown in Fig. 1. At 700 °C the data lie above the continuous parity line indicating that there was a tendency for the fuel-N in the parent coal to remain in the char under the conditions used in this study. However, at temperatures above 800 °C it is apparent that most of the data falls below the parity line, indicating a tendency for the nitrogen in the coal to be released as volatile-N.

3.2.1. Char petrographic characterization (see also Tables 5 and 6)

For the SA1 char, the proportions of the different char morphotypes apparently did not change significantly with temperature and the dominant morphotypes were tenuinetworks, mixed, and solids. However, at 900 and

Table 4
Ultimate char analysis (wt.%, d.b.) and H/C and N/C atomic ratio

Char	C	H	N	S	H/C	N/C
(Coal SA1, wt.% db)	72.22	4.45	1.88	0.69	0.73	0.022
SA1 700 °C	70.98	2.68	2.14	0.54	0.45	0.026
SA1 800 °C	74.69	1.92	2.17	0.55	0.31	0.025
SA1 900 °C	61.04	1.28	1.43	0.52	0.25	0.020
SA1 1000 °C	48.93	1.86	1.71	0.59	0.32	0.021
(Coal Col, wt.% db)	74.73	5.31	1.44	0.78	0.85	0.017
Col 700 °C	44.21	1.68	1.19	0.42	0.45	0.023
Col 800 °C	60.09	1.29	1.09	0.48	0.26	0.016
Col 900 °C	67.69	0.75	1.20	0.46	0.13	0.015
Col 1000 °C	54.60	0.70	1.32	0.48	0.15	0.021
Coal SA2, wt.% db	66.14	4.28	1.49	0.72	0.77	0.019
SA2 700 °C	74.80	2.00	1.80	n.d.	0.32	0.021
SA2 800 °C	34.30	0.70	0.70	n.d.	0.24	0.017
SA2 900 °C	75.80	1.30	1.60	n.d.	0.20	0.018
SA2 1000 °C	78.50	0.90	1.40	n.d.	0.21	0.015
(Coal SA3, wt.% db)	66.00	3.70	1.40	0.52	0.67	0.018
SA3 700 °C	72.90	1.90	1.60	n.d.	0.31	0.019
SA3 800 °C	71.60	1.30	1.40	n.d.	0.22	0.021
SA3 900 °C	67.90	1.00	1.30	n.d.	0.18	0.016
SA3 1000 °C	71.30	1.00	1.30	n.d.	0.22	0.016
(Coal EUA, wt.% db)	73.02	4.38	1.32	0.93	0.71	0.015
EUA 700 °C	65.78	1.33	1.41	0.57	0.24	0.018
EUA 800 °C	57.56	1.18	1.26	0.59	0.25	0.019
EUA 900 °C	55.87	1.05	1.00	0.46	0.22	0.015
EUA 1000 °C	36.98	0.64	0.55	0.35	0.21	0.013

n.d.: not determined.

Table 5
Petrographic char analysis (vol.%): individual values

Coal	T (°C)	T-sph$_1$	C-sph[2]	T-net[3]	C-net[4]	Mixed	Solid	F-Frag[5]	Uf-Frag[6]	Group 1[7]	Group2–3[8]
SA1	700	2	6	40	16	20	16	0	0	48	52
SA1	800	2	7	40	13	22	15	0	1	50	50
SA1	900	3	2	52	8	17	17	0	0	57	43
SA1	1000	1	4	58	6	19	12	0	0	63	37
Col	700	14	13	44	16	9	4	0	0	71	29
Col	800	16	15	46	13	6	1	4	1	80	21
Col	900	18	10	55	8	6	2	0	0	84	16
Col	1000	10	16	64	3	6	1	0	0	90	10
SA2	700	0	8	31	21	24	16	0	0	39	61
SA2	800	4	2	40	4	36	13	0	1	46	54
SA2	900	8	13	43	8	21	6	0	1	64	36
SA2	1000	3	9	50	9	24	4	1	0	63	37
SA3	700	4	5	18	6	33	34	0	0	27	73
SA3	800	3	2	36	6	30	21	2	0	43	57
SA3	900	10	4	37	9	29	11	0	0	51	49
SA3	1000	4	4	49	6	29	6	0	1	58	42
EUA	700	16	15	29	4	2	4	28	2	88	12
EUA	800	29	19	31	2	6	5	9	1	87	13
EUA	900	24	16	43	10	2	2	4	0	86	14
EUA	1000	13	14	60	7	2	2	1	2	88	12

[1]Tenuisphere; [2]Crassisphere; [3]Tenuinetwork; [4]Crassinetwork; [5]Fused fragment; [6]Unfused fragment;
[7](Tenuisphere + Crassisphere + Tenuinetwork + Fused fragment); [8](Crassinetwork + Mixed + Solid + Unfused fragment).

1000 °C, the volume of tenuinetworks was found to increase while the volume of crassinetworks decreased.

For the Col char, the volume of cenospheres and networks was very high. Additionally, there was not a significant variation of the cenospheres with the temperature, however, at 900 and 1000 °C the volume of tenuinetworks increased at the expense of the crassinetworks.

During Col coal petrographic analysis, the particles were found to be covered by fines, i.e., aggregates of clay and fine coal. As observed by scanning electron microscopy (SEM), devolatilization appears to lead to surrounding of organic matter by these fines. However, both optical microscopy images and the SEM micrographs are complementary and illustrate the way these fines seem to constrain the release of volatiles from the interior of the particle by deforming the cenospheres (Figs. 2 and 3).

For the SA2 char, the increase of the devolatilization temperature seems to enhance the formation of both mixed char and of tenuinetwork char morphotypes which could be attributed to the high volume of semifusinite present in this coal.

In the SA3 char, with increasing temperature, it was found that the proportion of solids decreased, the mixed chars were stable and the tenuinetworks increased. Apparently as temperature increased, there was a change of morphotypes from solids to mixed to tenuinetworks. However, large volumes of macrinoids and secretinoids are still observed, bearing the coal original composition.

The EUA coal produced a char of tenuispheres and tenuinetworks (Table 5).

The char morphotype classification in Group 1 (high porous chars) and Group 2–3 (mean and low porous chars) is also shown in Table 6. The comparison of these results with the devolatilization temperature of the chars is shown in Fig. 4. It can be seen that Col and EUA essentially produced high porous chars and that SA1, SA2, and SA3 yielded both Group 1 and Group 2–3 chars in almost equal amounts. However, with

Table 6
Petrographic char analysis (vol.%): mean values

	SA1	Col	SA2	SA3	EUA
Tenuisphere	2	15	4	5	20
Crassisphere	5	13	8	4	16
Tenuinetwork	48	52	41	35	41
Crassinetwork	11	10	11	7	6
Mixed	19	7	26	30	3
Solid[1]	15	2	10	18	3
Fused fragment	0	1	0	1	10
Unfused fragment	0	0	1	0	1
Cenosphere[2]	7	29	12	9	47
Group 1[3]	55	81	53	45	87
Group 2–3[4]	46	19	47	55	13

[1]Include inertoids, fusinoids, dense and solid forms.
[1]Tenuspheres + Crassispheres; [2]Tenuispheres + Crassispheres + Tenuinetworks + Fused fragments; [3]Crassispheres + Mixed + Solid + Unfused fragments.

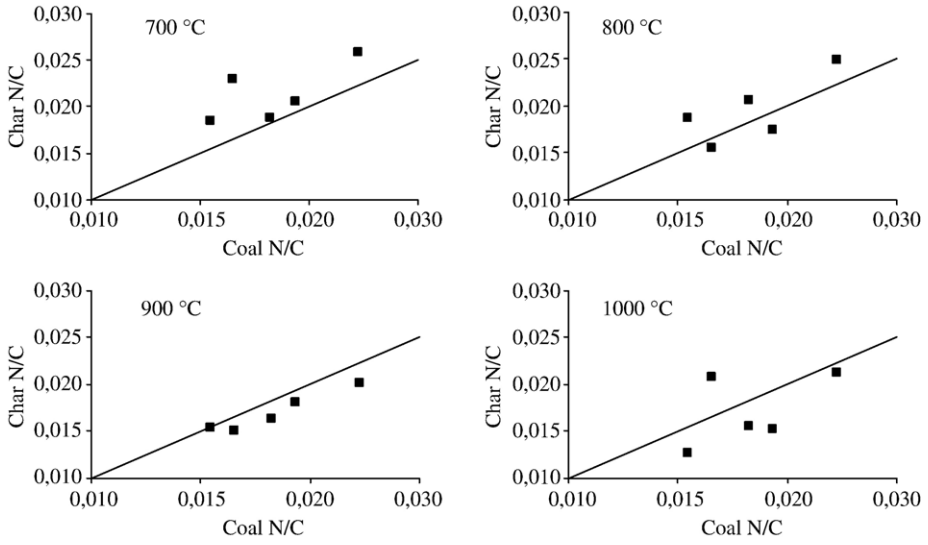

Fig. 1. Char N/C vs. coal N/C ratios for 700, 800, 900 and 1000 °C devolatilization trials.

temperature, there is a trend for the percentage of Group 1 chars to increase, except for EUA coal which seems to maintain the proportions between the two char groups considered.

3.3. Combustion measurements: NO and N_2O emissions

The results in Table 7 and in Fig. 5 show that the NO emissions from Col and EUA are generally lower than those found with SA1, SA2 and SA3. Furthermore, there seems to be a general tendency for NO emissions to decrease with combustion temperature in the case of the vitrinite-rich coals and to increase in the case of the inertinite-rich coals.

These results are consistent with other works (Pels et al., 1993; Boavida et al., 1996), in all cases, N_2O formation markedly decreases with the temperature. However, the N_2O emissions are, in general, lower for Col and EUA compared with SA1, SA2 and SA3 (Table 7 and Fig. 6).

4. Discussion and conclusions

The characterization results given in Table 4 and the N/C ratio for the chars and coals shown in Fig. 1 revealed that the nitrogen in coal was released with the volatile matter at greater amounts at higher temperatures during devolatilization. These results are consistent with previous works concerning the release of coal–nitrogen

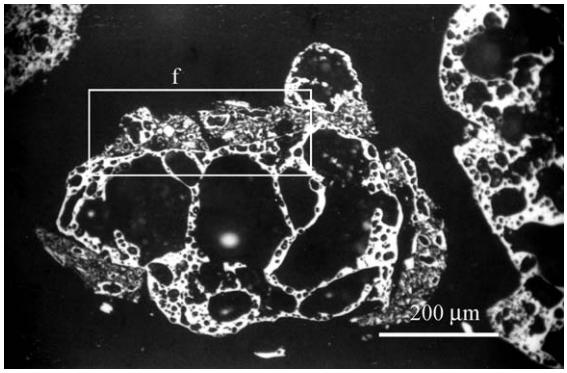

Fig. 2. Col 700 °C (Optical microscopy; N//): Tenuinetwork deformed by fines (f).

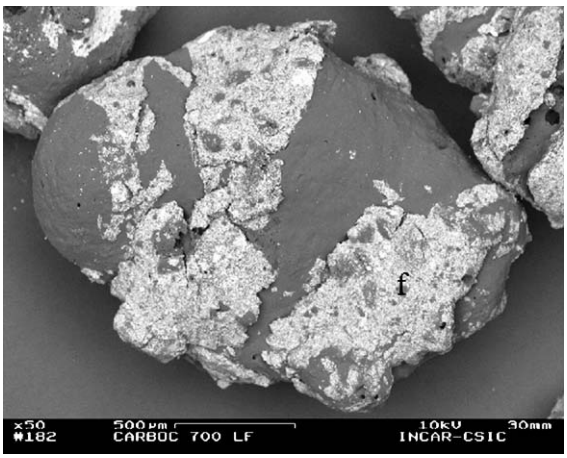

Fig. 3. Col 700 °C—SEM micrograph (×50; backscattered electron mode)—rounded and swelled particle covered by layers of fines (f) composed by organic and mineral matter.

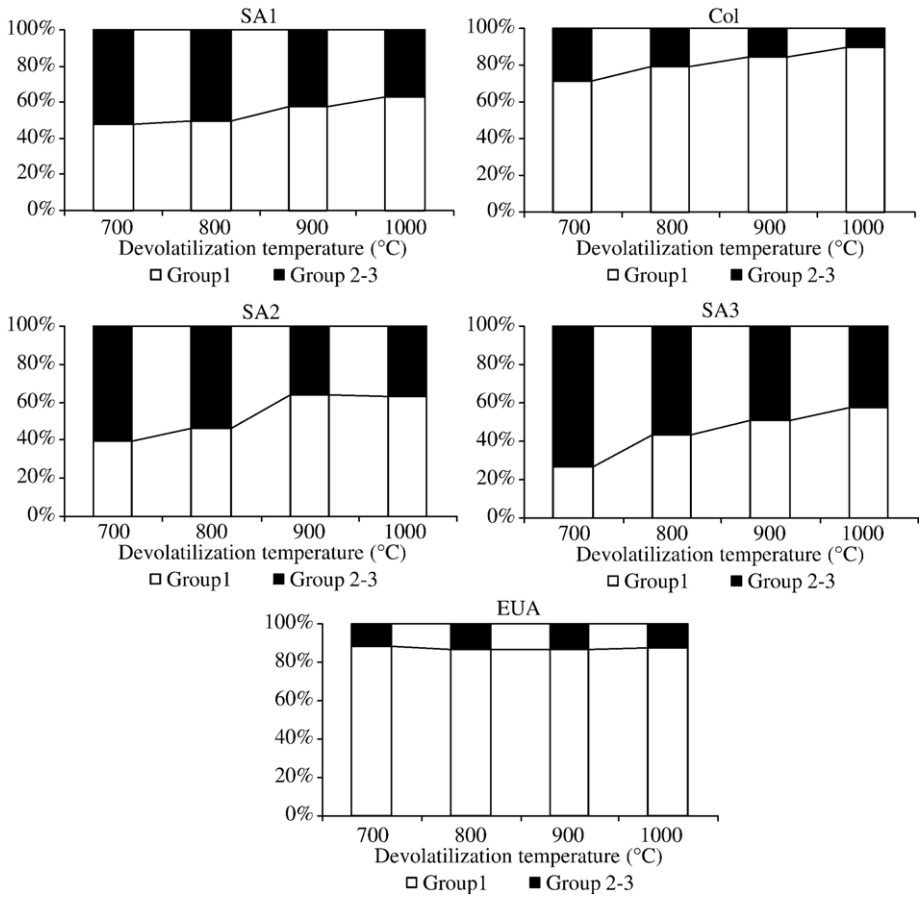

Fig. 4. Evolution of Group 1 and Group 2–3 char morphotypes with temperature (prepared in a FBC at 700–1000 °C; 10^4 K/s; 500–1000 μm).

during pyrolysis by various techniques (Brown and Thomas, 1993; Crelling et al., 1993; Gonzáles de Andrés and Thomas, 1994; Hayhurst and Lawrence, 1995). The work of Pohl and Sarofim referred to by Hayhurst and Lawrence (1995) illustrated that the fraction of fuel-N emitted during devolatilisation in a heated crucible increased with temperature: below 800 °C, less than 15% of the fuel-N left the coal; but, at around 900 °C, 40–50% of the nitrogen bound in the coal was released during devolatilization. Hayhurst and Lawrence (1995) found that the only parameter to influence the amount of fuel-N released during FBC devolatilization or pyrolysis was temperature of the bed. By increasing the bed temperature from 750 to 900 °C they claimed that the fraction of fuel-N released increased by 80–90%, on average.

Other combustion parameters such as higher heating rates and lower particle size, simulating p.f. conditions, are also responsible for higher quantities of nitrogen liberated in volatiles from the coal (Harding et al., 1996).

Other coal properties, such as the maceral composition, also appear to influence the nitrogen release from coals. Crelling et al. (1993) performed programmed temperature studies in an Entrained Flow Reactor (EFR) with chars (1273 ± 5 K) from maceral concentrates and found that the maceral composition was responsible for variations in the retention of nitrogen in the chars, i.e., they found that the nitrogen increased in the pyrolysis chars, by about 25–30% compared to the whole coal with vitrain samples and by about 65–75% in the case of fusain samples.

Due to the inability to perform micro-proximate analyses in the chars in this study, our results are presented only on a dry basis, implying, because the chars had sand embedded in their surfaces, any small error in the determination of the ultimate analysis of the char was amplified (Hayhurst and Lawrence, 1995).

The plastic properties of the vitrinite macerals were demonstrated under the FBC conditions used in this study in the production of greater amounts of high porous chars from the vitrinite-rich coals. On the other

Table 7
NO and N_2O coal combustion emissions (values in ppm, referred to 6% O_2; sand bed weight: 400 g; fluidization air pressure: 1 bar; fluidization air flow rate: 14 dm^3/min; coal feed rate: 1.2 g/min; coal particle sizes: 500–1000 μm)

	SA1	Col	SA2	SA3	EUA
Temperature (°C)					
NO emissions					
700	225	186	185	219	112
800	231	210	517	328	145
900	285	133	488	320	132
1000	275	63	514	357	133
Mean values	254	148	426	306	130
N_2O emissions					
700	148	36	55	7	33
800	108	33	45	33	25
900	43	23	38	40	18
1000	26	21	32	28	18
Mean values	81	29	42	27	24
$Mean_{700–800}$	128	35	50	20	29
$Mean_{900–1000}$	34	22	35	34	18

hand, inertinite macerals with less plasticity were responsible for the higher amounts of solid char morphotypes. Similar observations were reported by other authors for FBC conditions (Vleeskens and Nandi, 1986; Vleeskens et al., 1988; Ross et al., 2000).

Under p.f. conditions it was also observed that the inertinites underwent through thermoplasticity development accompanied by lower porosity compared with vitrinites, resulting in greater percentages of solid structures originating from high-reflectance inertinite-rich coals. But, in this case, the structure of the resulting char particles mainly depends on the individual maceral composition of the parent coal particles (Alonso et al., 2001; Chen and Ma, 2002; Yu et al., 2003).

The reclassification of the chars in Group I (tenuispheres, crassispheres and tenuinetworks) and Group II (crassinetwork, mixed and solids) (Bailey, 1994; Diessel, 1998) revealed that the Col and EUA coals essentially produced Group I and both types of char morphotype groups were obtained from SA1, SA2 and SA3 coals. However, at 900 and 1000 °C SA1, SA2 and SA3 were also able to produce high volumes of Group I chars.

Temperature seems to significantly influence the morphology of the char obtained under the FBC conditions used in this study. That was previously concluded by other authors for p.f. conditions simulated in a drop tube furnace (DTF) (Alonso et al., 2001). In those cases, the authors found that the greater release of volatiles at the higher temperature was likely to lead to a more cenospheric or networked char.

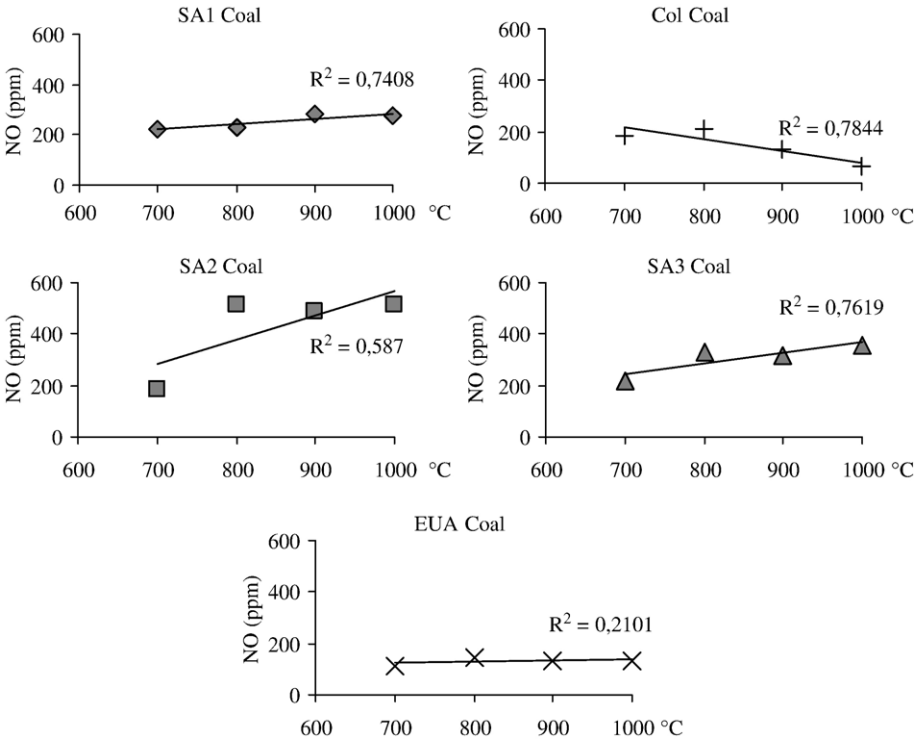

Fig. 5. NO emissions at different FBC temperatures (700–1000 °C) for the five coals studied.

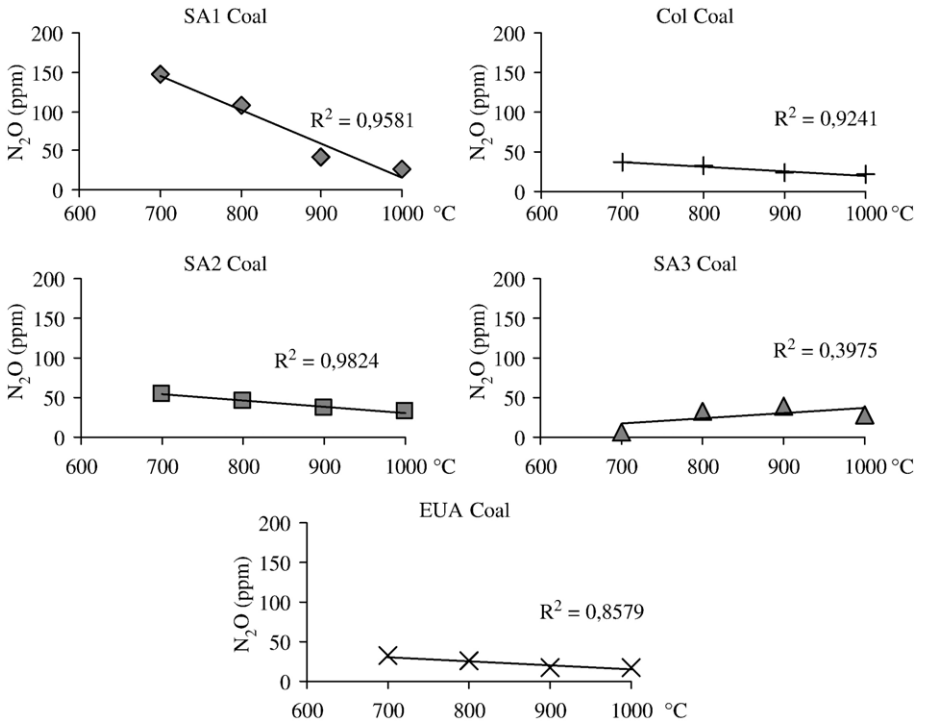

Fig. 6. N_2O emissions at different FBC temperatures (700–1000 °C) for the five coals studied.

Under the FBC conditions used in this study, as the reaction to temperature increased it is probable that semifusinite became more reactive and thermoplastic, thus releasing more volatile matter. This led to a rise in the amount of tenuineworks, while vitrinite macerals always produced cenospheres or tenuinetworks for all temperatures. On the other hand, the high reflectance inertinite macerals such as fusinite, secretinite, and macrinite essentially formed solid char morphotypes.

In the case of Col coal char morphotypes, the increase of the tenuinetworks at the expense of the crassinetworks may be explained by the stronger secondary devolatilization occurring at the char walls.

In fact, at high temperatures (900 and 1000 °C) the fused char walls became thinner with very large pores leading to a tenuinetwork configuration. However, at the same time particles that eventually would be shaped as mixed and solids at lower temperatures evolve to crassinetworks at high temperatures. What happens is that inertinite macerals seems to react more only at high temperatures (Valentim et al., 2004).

An additional factor determining char morphology could be the coal micro-stratification because in an FBC system the particles size used are larger than in p.f. Hence, the network morphology could be enhanced due to the existence of several micro-layers of vitrinite in the same coal particle entering the furnace chamber (Valentim et al., 2006-this volume).

Because the coals used are all high volatile bituminous, no major structural variations between the chars originating from the reactive macerals in parent coals were expected. The optical microscopic characterization revealed that fused chars had only a basic anisotropy but no clearly visible coke structures were found, apart from those on the edges of semifusinite macerals. The high reflectance inertinite macerals remained isotropic. Harding et al. (1996) found, for chars prepared in an Entrained Flow Reactor simulating p.f. conditions, that the increased extent of structural orientation could be associated with a decrease in the porosity in the anistropic chars. The same work claimed that the extent of the reduction in NO varied with the temperature, mass transport and the structure of the char.

The nitrogen oxides emissions resulting from FBC of the five coals used in this study were plotted against the trial temperatures, the maceral composition and the char morphology. These relations revealed that as the temperature rose, the NO emissions decreased for the vitrinite-rich coals and increased in the case of the inertinite-rich coals. Additionally, the lowest NO and N_2O emissions were seen to be associated with the vitrinite-rich coals and the highly porous char morphotypes produced by vitrinite. Finally, as expected, N_2O

decreased with temperature. These observations agree well with other studies of several authors that used EFR and temperature programmed trials to study the behavior of coals, maceral concentrates and their chars. Armesto et al., (2003), also included the Colombian coal in their FBC studies and reach to similar results.

Crelling et al. (1993) concluded that variations both in lithotype and maceral composition gave rise to large variations in nitrogen content, char morphology and reactivity, i.e., that although the nitrogen content decreased in the order: vitrinite > semifusinite > inertinite, the conversion of the coal and char nitrogen to NO showed the reverse order: fusinite > semifusinite > vitrinite. Other authors also concluded that there could be other factors related to the structure and properties of the coal, in addition to the combustion conditions, such as rank and the degree of surface oxidation (Shimizu et al., 1992; Gavin and Dorrington, 1993; Pels et al., 1993), maceral composition (Gonzáles de Andrés and Thomas, 1994; Wang et al., 1994), mineral matter (Zhao et al., 2003), char reactivity, and surface area (Kilpinen et al., 2002; Shen et al., 2003; Zhao et al., 2003).

In summary, nitrogen was released from the coal as the trial temperature increased.

The variations in the coal maceral and microlithotype composition influenced the char morphotypes generated under the FBC conditions used in this study, i.e., vitrinite-rich coals produced high amounts of highly porous chars while inertinite-rich coals were responsible for the formation of high amounts of low-porosity chars.

The NO emissions from vitrinite-rich coals decreased with temperature while inertinite-rich coals revealed the opposite tendency.

The lower amounts of NO and N_2O were released from the vitrinite-rich coals and are also related with the highly porous char morphotypes produced by these coals.

Acknowledgements

The authors thank the Fundação para a Ciência e a Tecnologia (Portugal; grant BPD/5530/2001) and the ECSC for financing the Project, Contract 7220-ED/068.

References

Alonso, M.J.G., Borrego, A.G., Álvarez, D., Kalkreuth, W., Menéndez, R., 2001. Physicochemical transformations of coal particles during pyrolysis and combustion. Fuel 80, 1857–1870.

Álvarez, D., 1996. Estructura del char y su influencia sobre la combustión del carbón. Ph.D. Thesis. Universidad de Oviedo. Oviedo.

Álvarez, D., Borrego, A.G., Menéndez, R., 1997. Unbiased methods for the morphological description of char structures. Fuel 76, 1241–1248.

Armesto, L., Boerrigter, H., Bahillo, A., Otero, J., 2003. N_2O emissions from fluidised bed combustion. The effect of fuel characteristics and operating conditions. Fuel 82, 1845–1850.

Bailey, J.G., 1994. Predicting unburnt carbon and tracing coal components in thermal blends. White paper of the Working Group on Environmental Applications of Coal Petrography. 46th. Annual Meeting of the International Committee for Coal and Organic Petrology (ICCP), Oviedo, pp. 17–18.

Bailey, J.G., Tate, A., Diessel, C.F.K., Wall, T.F., 1990. A char morphology system with applications to coal combustion. Fuel 69, 225–239.

Boavida, D., Gulyurtlu, I., Lobo, L.S., Cabrita, I., 1996. N_2O formation during coal combustion in fluidized beds—is it controlled by homogeneous or heterogeneous reactions? Energy Convers. Manag. 37, 1271–1278.

Brown, S.D., Thomas, K.M., 1993. A comparison of NO release from coals and entrained-flow reactor chars during temperature-programmed combustion. Fuel 72, 359–365.

Burchill, P., Welch, L.S., 1989. Variation of nitrogen content and functionality with rank for some UK bituminous coals. Fuel 68, 100–104.

Chen, P., Ma, J., 2002. Petrographic characteristics of Chinese coals and their application in coal utilization processes. Fuel 81, 1389–1395.

Crelling, J.C., Thomas, K.M., Marsh, H., 1993. The release of nitrogen and sulphur during the combustion of chars derived from lithotypes and maceral concentrates. Fuel 72, 349–357.

Damberger, H.H., Harvey, R.D., Ruch, R.R., Thomas Jr., J., 1984. The Science and Technology of Coal and Coal Utilization. London, Plenum Press, New York (N.Y.), pp. 7–45.

Diessel, C.F.K., 1998. Technological applications. In: Taylor, A. (Ed.), Organic Petrology. Gebrüder Borntraeger, Berlin, Stuttgart, pp. 519–614.

Gavin, D.G., Dorrington, M.A., 1993. Factors in the conversion of fuel nitrogen to nitric and nitrous oxides during fluidised bed combustion. Fuel 72, 381.

Gonzáles de Andrés, A.I., Thomas, K.M., 1994. The influence of mineral matter and carbonization conditions on nitrogen release during coal combustion. Fuel 73, 635–641.

Harding, A.W., Brown, S.D., Thomas, K.M., 1996. Release of NO from the combustion of coal chars. Combustion and Flame 107, 336–350.

Hayhurst, A.N., Lawrence, A.D., 1995. The devolatilization of coal and a comparison of chars produced in oxidizing and inert atmospheres in fluidised beds. Combustion and Flame 100, 591–604.

Hindmarsh, C.J., Wang, W., Thomas, K.M., Crelling, J.C., 1994. The release of nitrogen during the combustion of macerals, micro-lithotypes and their chars. Fuel 73, 1229–1234.

IEA/OECD 1999. Cleaner coal technologies: options. International Energy Agency, Department of Trade and Industry, p. 28.

Jacobson, M.Z., 2002. Atmospheric Pollution: History, Science and Regulation. Cambridge University Press, Cambridge, UK, p. 399.

Kilpinen, P., Kallio, S., Konttinen, J., Barisic, V., 2002. Char-nitrogen oxidation under fluidised bed combustion conditions: single particle studies. Fuel 81, 2349–2362.

Molina, A., Eddings, E.G., Pershing, D.W., Sarofim, A.F., 2000. Char nitrogen conversion: implications to emissions from coal-fired utility boilers. Progr. Energy Comb. Sci. 26, 507–531.

Pels, J.R., Wójtowicz, M.A., Moulijn, J.A., 1993. Rank dependence of N_2O emission in fluidised-bed combustion of coal. Fuel 72, 373–379.

Rosenberg, P., Petersen, H.I., Thomsen, E., 1996. Combustion char morphology related to combustion temperature and coal petrography. Fuel 75, 1071–1082.

Ross, D.P., Heidenreich, C.A., Zhang, D.K., 2000. Devolatilisation times of coal particles in a fluidised-bed. Fuel 79, 873–883.

Shen, B.X., Mi, T., Liu, D.C., Feng, B., Yao, O., Winter, F., 2003. N_2O emission under fluidized bed combustion condition. Fuel Process. Technol. 84, 13–21.

Shimizu, T., Sazawa, Y., Adschiri, T., Furusawa, T., 1992. Conversion of char-bound nitrogen to nitric oxide during combustion. Fuel 71, 361–365.

Sørensen, H.S., Rosenberg, P., Petersen, H.I., Sørensen, L.H., 2000. Char porosity characterisation by scanning electron microscopy and image analysis. Fuel 79, 1379–1388.

Valentim, B., Lemos de Sousa, M.J., Abelha, P., Boavida, D., Gulyurtlu, I., 2004. Relation between the petrographic composition of coal and the morphology of pyrolysis char produced in fluidised bed. Energy Fuels 18, 611–618.

Valentim, B., Lemos de Sousa, M.J., Abelha, P., Boavida, D., Gulyurtlu, I., 2006-this volume. The identification of unusual microscopic features in coal and their derived chars: influence on coal fluidised bed combustion. Int. J. Coal Geol. 67, 202–211. doi:10.1016/j.coal.2005.11.003.

Varey, J.E., Hindmarsh, C.J., Thomas, K.M., 1996. The detection of reactive intermediates in the combustion and pyrolysis of coals, chars and macerals. Fuel 75, 164–176.

Vleeskens, J.M., Nandi, N., 1986. Burnout of coals. Comparative bench-scale experiments on pulverized fuel and fluidised bed combustion. Fuel 65, 797–802.

Vleeskens, J.M., van Haasteren, T.W.M.B., Roos, M., Gerrits, J., 1988. Behaviour of different char components in fluidised bed combustion: a char petrography study. Fuel 67, 426–430.

Wang, W., Brown, S.D., Hindmarsh, C.J., Thomas, K.M., 1994. NO_x release and reactivity of chars from a wide range of coals during combustion. Fuel 72, 1381–1388.

Xie, Z., Feng, J., Zhao, W., Xie, K.-C., Pratt, K.C., Li, C.-Z., 2001. Formation of NO_x and SO_x precursors during the pyrolisis of coal and biomass: Part IV. Pyrolisis of a set of Australian and Chinese coals. Fuel 80, 2131–2138.

Yu, J., Strezov, V., Lucas, J., Terry Wall, T., 2003. Swelling behaviour of individual coal particles in the single particle reactor. Fuel 82, 1977–1987.

Zhao, Z., Qiu, J., Li, W., Chen, H., Li, B., 2003. Influence of mineral matter in coal on decomposition of NO over coal chars and emission of NO during char combustion. Fuel 82, 949–957.